Suppression of age-related salivary gland autoimmunity by glycosylation-dependent galectin-1-driven immune inhibitory circuits

Verónica C. Martínez Allo[a], Vanesa Hauk[b,1], Nicolas Sarbia[a,1], Nicolás A. Pinto[a], Diego O. Croci[c], Tomás Dalotto-Moreno[a], Rosa M. Morales[a], Sabrina G. Gatto[a], Montana N. Manselle Cocco[a], Juan C. Stupirski[a], Ángel Deladoey[d], Esteban Maronna[e], Priscila Marcaida[f], Virginia Durigan[f], Anastasia Secco[f], Marta Mamani[f], Alicia Dos Santos[d], Antonio Catalán Pellet[f], Claudia Pérez Leiros[b], Gabriel A. Rabinovich[a,g,2,3], and Marta A. Toscano[a,2,3]

[a]Laboratorio de Inmunopatología. Instituto de Biología y Medicina Experimental (IBYME), Consejo Nacional de Investigaciones Científicas y Técnicas (CONICET), C1428, Ciudad de Buenos Aires, Argentina; [b]Instituto de Química Biológica de la Facultad de Ciencias Exactas y Naturales (IQUIBICEN), CONICET, Universidad de Buenos Aires, C1428, Ciudad de Buenos Aires, Argentina; [c]Instituto de Histología y Embriología de Mendoza (IHEM), CONICET, Facultad de Ciencias Exactas y Naturales, Universidad Nacional de Cuyo, C5500, Mendoza, Argentina; [d]División de Patología, Hospital Bernardino Rivadavia, C1425, Ciudad de Buenos Aires, Argentina; [e]Servicio de Patología, Sanatorio Mater Dei, C1425, Ciudad de Buenos Aires, Argentina; [f]División de Reumatología, Hospital Bernardino Rivadavia, C1425, Ciudad de Buenos Aires, Argentina; and [g]Facultad de Ciencias Exactas y Naturales, Universidad de Buenos Aires, C1428, Ciudad de Buenos Aires, Argentina

Contributed by Gabriel A. Rabinovich, February 7, 2020 (sent for review December 30, 2019; reviewed by Brian A. Cobb and Naoyuki Taniguchi)

Aging elicits quantitative and qualitative changes in different immune components, leading to disruption of tolerogenic circuits and development of autoimmune disorders. Galectin-1 (Gal1), an endogenous glycan-binding protein, has emerged as a regulator of immune cell homeostasis by shaping the fate of myeloid and lymphoid cells. Here, we demonstrate that aged Gal1-null mutant (*Lgals1*$^{-/-}$) mice develop a spontaneous inflammatory process in salivary glands that resembles Sjögren's syndrome. This spontaneous autoimmune phenotype was recapitulated in mice lacking β1,6N-acetylglucosaminyltransferase V (Mgat5), an enzyme responsible for generating β1,6-branched complex N-glycans, which serve as a major ligand for this lectin. Lack of Gal1 resulted in CD11c^{+} dendritic cells (DCs) with higher immunogenic potential, lower frequency of Foxp3^{+} regulatory T cells (Tregs), and increased number of CD8^{+} T cells with greater effector capacity. Supporting its tolerogenic activity, Gal1 expression decreased with age in autoimmunity-prone nonobese diabetic (NOD) mice. Treatment with recombinant Gal1 restored tolerogenic mechanisms and reduced salivary gland inflammation. Accordingly, labial biopsies from primary Sjögren's syndrome patients showed reduced Gal1 expression concomitant with higher number of infiltrating CD8^{+} T cells. Thus, endogenous Gal1 serves as a homeostatic rheostat that safeguards immune tolerance and prevents age-dependent development of spontaneous autoimmunity.

autoimmunity | inflammation | Sjögren's syndrome | galectin-1 | N-glycans

Immune tolerance relies on regulatory circuits responsible for avoiding autoimmune reactions and dampening exacerbated immune responses to prevent tissue damage. These homeostatic mechanisms require the interplay of immune cell mediators promoting contraction of innate and adaptive immune compartments after the completion of immune responses (1). However, the presence of self-reactive immune cells within the lymphocyte repertoire entails an intrinsic potential of triggering autoimmune reactions, whose development and perpetuation will depend on genetic and environmental cues leading to disruption of regulatory networks and breakdown of immune tolerance (1, 2).

The mechanisms responsible for sustaining peripheral T-cell tolerance involve the expression and activation of several regulatory pathways, including coinhibitory receptors and ligands, so-called immune checkpoints (i.e., CTLA-4/ B7.1-B7.2; PD-1/PD-L1; BTLA/ HVEM), lineage-specific transcription factors (i.e., Foxp3), and immunoregulatory cytokines (i.e., IL-10, TGF-β_1). The use of genetically modified mouse strains has provided important clues on the critical role of these regulatory networks in safeguarding immune tolerance and preventing autoimmune diseases. In fact, lack of key immune silencers such as CTLA-4, Foxp3, and TGFβ_1 led to severe lymphoproliferative disorders with major infiltration of central organs and death within the first weeks of age (3–5). However, other central tolerogenic pathways including those involving PD-1 and BTLA showed a more restricted regulatory function and may be categorized as rheostats of immune responses since their deficiency leads to age-dependent tissue-specific immunopathology (6–8).

Galectins have emerged as a family of soluble glycan-binding proteins capable of regulating a broad range of biological processes. They are defined by a common structural fold and a

Significance

Different immune inhibitory circuits act in concert to prevent and limit the extent of deleterious autoimmune reactions occurring during the aging process. An in-depth understanding of these pathways is critical for implementation of more selective and powerful immunomodulatory modalities capable of attenuating autoimmune inflammation. Here we show that lack of galectin-1 (an endogenous β-galactoside-binding protein) or specific N-glycosylated ligands leads to a gradual breakdown of tolerogenic programs and to the establishment of age-related salivary gland autoimmunity. This study emphasizes the role of lectin–glycan interactions in the maintenance and restoration of immune tolerance and highlights their clinical relevance and therapeutic potential in chronic inflammatory disorders.

Author contributions: V.C.M.A., A.C.P., C.P.L., G.A.R., and M.A.T. designed research; V.C.M.A., V.H., N.S., N.A.P., D.O.C., T.D.-M., R.M.M., S.G.G., M.N.M.C., J.C.S., Á.D., E.M., P.M., V.D., A.S., and M.A.T. performed research; M.M., A.D.S., A.C.P., C.P.L., G.A.R., and M.A.T. contributed new reagents/analytic tools; V.C.M.A., V.H., N.S., N.A.P., D.O.C., T.D.-M., Á.D., E.M., P.M., V.D., A.S., A.C.P., C.P.L., G.A.R., and M.A.T. analyzed data; and V.C.M.A., G.A.R., and M.A.T. wrote the paper.

Reviewers: B.A.C., Case Western Reserve University School of Medicine; and N.T., Osaka International Cancer Institute.

The authors declare no competing interest.

[1]V.H. and N.S. contributed equally to this work.

[2]G.A.R. and M.A.T. contributed equally to this work.

[3]To whom correspondence may be addressed. Email: gabyrabi@gmail.com or martalitos@gmail.com.

This article contains supporting information online at https://www.pnas.org/lookup/suppl/doi:10.1073/pnas.1922778117/-/DCSupplemental.

First published March 11, 2020.

highly conserved carbohydrate recognition domain (CRD) (9). These endogenous lectins are synthesized as cytosolic proteins and can be secreted to the extracellular milieu through a nonconventional endoplasmic reticulum (ER)-Golgi–independent route (10). Galectin-1 (Gal1), a prototype member of this family, has emerged as a regulator of immune cell homeostasis (11, 12). Extracellularly, this lectin acts by recognizing N-acetyllactosamine (LacNAc) residues in complex N-glycans and core 2-O-glycans on a variety of cell surface receptors including CD45, CD43, and CD7 (13). In vivo administration of recombinant Gal1 or its genetic delivery suppressed clinical manifestations of autoimmune inflammation in several models including experimental autoimmune encephalomyelitis (14, 15), collagen-induced arthritis (16), Con A-induced hepatitis (17), trinitrobenzene sulfonic acid (TNBS)-induced colitis (18), nephrotoxic serum nephritis (19), experimental autoimmune uveitis (20), autoimmune diabetes (21), and autoimmune orchitis (22). The proposed mechanisms underlying these immunomodulatory effects include a bias toward Th2 cytokine production (16, 20), expansion of regulatory T cells (Tregs) (20), apoptosis of activated Th1 and Th17 effector cells (14, 23–25), differentiation of tolerogenic dendritic cells (DCs) (26), exposure of phosphatidylserine in neutrophils leading to their removal by phagocytes (27), and polarization of macrophages and microglia toward an M2 phenotype (28, 29). Accordingly, mice lacking Gal1 (*Lgals1*$^{-/-}$) displayed enhanced T-cell activation and increased tissue damage in established models of autoimmune encephalomyelitis, arthritis, and lupus-like disease (14, 29–31). However, despite considerable progress, the immunological consequences of disrupting endogenous Gal1 have not been explored in nonprone nonimmunized mice.

Sjögren's syndrome is among the most frequent systemic autoimmune diseases, affecting primarily women, with an estimated prevalence of 0.1–4.8% of the population (32). This systemic autoimmune disease affects mainly exocrine glands and is usually associated with persistent oral and ocular dryness due to functional damage of affected organs. Sjögren's syndrome can occur as primary disease (i.e., pSS) with clinical manifestations ranging from sicca symptoms to extraglandular systemic signs or can be associated to other autoimmune diseases such as systemic lupus erythematosus (SLE) and rheumatoid arthritis (secondary Sjögren's syndrome; sSS) (32, 33). This autoimmune exocrinopathy is characterized by focal lymphocytic infiltration and the presence of several autoantibodies including antinuclear antibodies (ANA), rheumatoid factor, and antibodies recognizing Ro/SSA and/or La/SSB (33–37). Thus far, the etiopathogenic mechanisms of Sjögren's syndrome have not been fully elucidated.

In the present study, we analyzed the hierarchical role of Gal1 and specific N-glycans in the development of spontaneous autoimmunity and evaluated central pathways underlying this immunological phenotype. Aged *Lgals1*$^{-/-}$ mice developed a spontaneous inflammatory disorder that recapitulated human Sjögren's syndrome via the coordinated amplification of both innate and adaptive immune pathways. This effect was mirrored in aged *Mgat5*$^{-/-}$ mice lacking complex branched N-glycans, which serve as major Gal1 ligands. Supporting these findings, we found a negative association between Gal1 expression and infiltration of CD8$^+$ T cells in labial biopsies from patients with primary Sjögren's syndrome. Thus, loss of Gal1 disrupts tolerogenic circuits, leading to a gradual breakdown of immune tolerance mechanisms and establishment of age-related spontaneous autoimmunity, highlighting the relevance of this endogenous lectin as a possible therapeutic agent in autoimmune diseases.

Results

Disruption of Gal1 Expression or N-Glycan Branching Leads to the Development of Spontaneous Sialadenitis. Since aging confers increased susceptibility to development of autoimmune diseases, we studied the role of Gal1 in the control of immune tolerance in aged (≥9 mo old) *Lgals1*$^{-/-}$ mice. We first determined the presence of autoantibodies in serum samples and the composition of immune cell infiltrates in several tissues and organs. We found that aged *Lgals1*$^{-/-}$ mice show increased levels of anti-dsDNA, anti-nuclear (ANA), and anti-Ro/SSA autoantibodies when compared to age-matched wild-type (WT) mice (Fig. 1*A*). Moreover, serum samples of aged *Lgals1*$^{-/-}$ mice showed increased reactivity against nuclear structures in HEp-2 cells, with a homogenous and dense speckled pattern consistent with that triggered by anti-DNA, anti-Ro/SSA, and anti-La/SSB autoantibodies (Fig. 1*B*). The presence of autoantibodies suggests the possibility that autoimmune inflammatory processes may occur in particular tissues and organs. Histopathological assessment revealed the presence of conspicuous mononuclear cell infiltration in salivary glands of aged *Lgals1*$^{-/-}$ mice. The magnitude of histopathological signs was determined following Chisholm and Mason's criteria (38). We found that *Lgals1*$^{-/-}$ mice displayed increased inflammatory score compared to WT counterparts (Fig. 1*C*). The increased inflammatory process was associated with elevated salivary gland weight and alterations of the tissue architecture, evidenced by the loss of acinar area with an increased number of ducts per unit area (Fig. 1 *D* and *E*). Next, we examined the composition of the immune cell infiltrates in the salivary gland and found that *Lgals1*$^{-/-}$ mice had an increased percentage of CD45$^+$ infiltrating leukocytes with a significant rise in the frequency of CD3$^+$CD8$^+$ T cells as compared to WT mice (Fig. 1*F*). However, we found no significant differences in the frequency of CD3$^+$CD4$^+$ T cells or B220$^+$ B cells (Fig. 1*F*). Histopathological analysis of other tissues and organs including kidney, skin, stomach, retina, thyroid gland, pancreas, liver, and uterus revealed no significant alterations in the magnitude of immune cell infiltration as compared to aged C57BL/6 WT mice (*SI Appendix*, Fig. S1).

N-acetyllactosamine residues present in complex N-glycans serve as major ligands for Gal1. In particular, the enzyme β1,6 N-acetylglucosaminyltransferase 5 (Mgat5), which catalyzes the synthesis of β1,6 N-acetylglucosamine branched N-glycans, is central for the biosynthesis of Gal1 ligands. To gain a more integrated picture of the role of Gal1–glycan interactions during aging, we analyzed the presence of salivary gland inflammation in *Mgat5*$^{-/-}$ mice and found that, similar to *Lgals1*$^{-/-}$ mice, aged *Mgat5*$^{-/-}$ mice displayed augmented inflammatory scores, increased salivary gland weight, and altered glandular structure (Fig. 2 *A*–*C*). Consistent with these findings, salivary glands from *Mgat5*$^{-/-}$ mice also showed higher infiltration of CD45$^+$ cells. Interestingly, these mice showed a significant increase in all of the three lymphocyte populations analyzed (Fig. 2*D*). Thus, deficiency in Gal1 or specific glycosylated ligands leads to the development of an inflammatory autoimmune process that affects salivary glands and resembles Sjögren's syndrome in humans.

***Lgals1*$^{-/-}$ Mice Display Augmented CD8$^+$ T Cell Function in Salivary Glands.** To better understand the cellular components underlying salivary gland inflammation in aged *Lgals1*$^{-/-}$ mice, we immunophenotyped infiltrating CD8$^+$ T cells and found a greater proportion of CD8$^+$IL-2$^+$IFN-γ$^+$ and CD8$^+$IFN-γ$^+$ cells in salivary glands from aged *Lgals1*$^{-/-}$ compared to control mice (Fig. 3*A*), suggesting a role for Gal1 in regulating the effector function of infiltrating CD8$^+$ T cells. In addition, we found a higher percentage of CD8$^+$PD-1$^+$ lymphocytes in the salivary glands of *Lgals1*$^{-/-}$ versus WT mice (Fig. 3*B*). To investigate whether Gal1 deficiency impacts the integrity of the PD-1/PD-L1 axis, we then analyzed expression of the coinhibitory ligand PD-L1 in salivary glands. We found that aged *Lgals1*$^{-/-}$ mice expressed significantly lower levels of PD-L1 than age-matched WT mice (Fig. 3*C*), suggesting that, in the absence of Gal1, CD8$^+$PD-1$^+$ cells would meet a less inhibitory milieu within the salivary gland. To gain further insight into the mechanisms involved in tissue infiltration and damage, we evaluated the expression of chemokines and chemokine

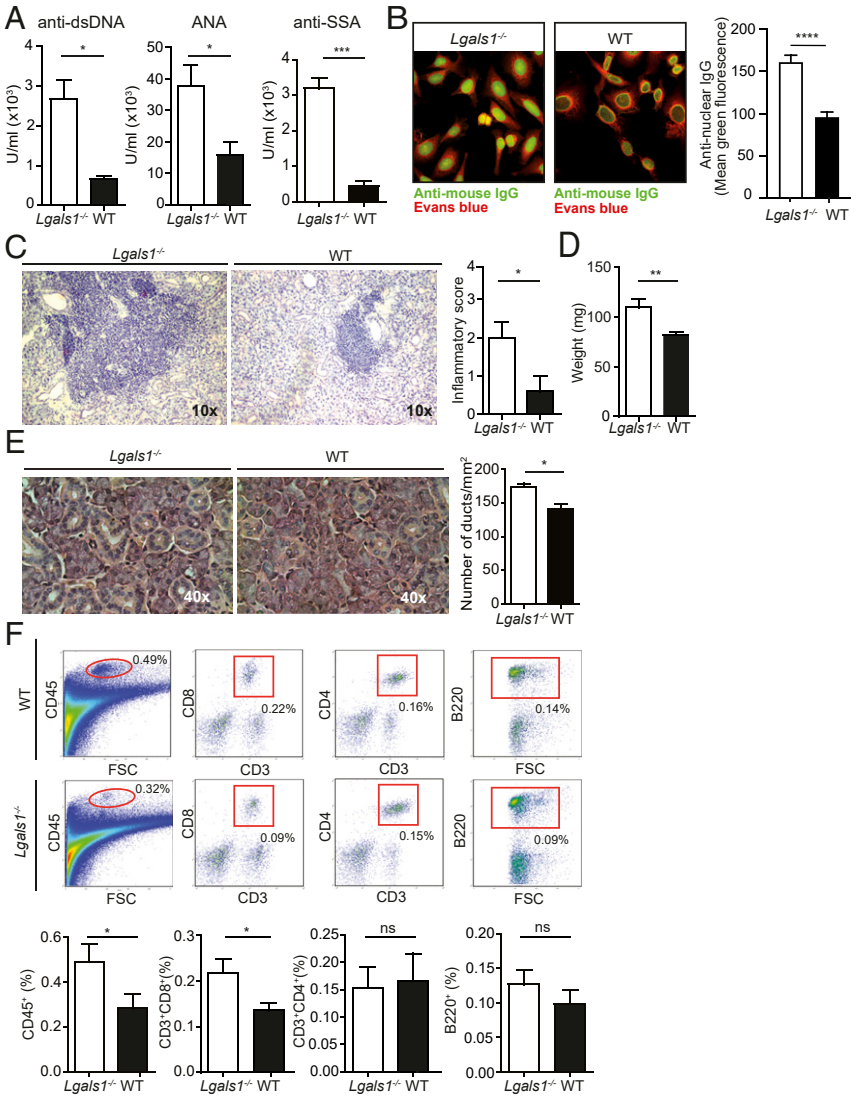

Fig. 1. Aged *Lgals1*$^{-/-}$ mice develop spontaneous sialadenitis. (*A* and *B*) Quantitative and qualitative detection of autoantibodies in sera from aged *Lgals1*$^{-/-}$ and WT mice. (*A*) ELISA of anti-dsDNA, anti-ANA, and anti-SSA in serum samples from aged mice (mean ± SEM, $n = 6$). (*B*, *Left*) Indirect immunofluorescence on HEp-2 cells exposed to serum from aged mice (representative results from five independent experiments with $n = 3$ per experiment). (*B*, *Right*) Quantification of anti-nuclear IgG (mean ± SEM). (*C*–*E*) Analysis of submandibular salivary glands from aged (≥9 mo) *Lgals1*$^{-/-}$ and WT mice. (*Left*) Representative images of salivary gland tissue sections (hematoxylin); (*Right*) inflammatory score determined as described in *Materials and Methods* ($n = 8$; *C*). Weight (mean ± SEM, $n = 8$; *D*) and number of ducts per square millimeter (mean ± SEM, $n = 5$; *E*, *Left*, representative H&E images; *E*, *Right*, quantification) of submandibular salivary glands. (*F*) Inflammatory infiltrates in salivary glands of aged *Lgals1*$^{-/-}$ and WT mice determined by flow cytometry. (*Upper*) Representative dot plots showing gating strategies used to quantify the frequency of CD45$^+$, CD3$^+$CD8$^+$, CD3$^+$CD4$^+$, and B220$^+$ cells. The value shown in the graph represents the percentage of infiltrating cells with respect to the whole salivary gland cells. (*Lower*) The average percentage of infiltrating cell populations of the whole salivary gland (mean ± SEM, $n = 16$). *$P < 0.05$; **$P < 0.01$; ***$P < 0.001$; ****$P < 0.0001$, Student's *t* test.

receptors responsible for recruiting CD8$^+$ effector T cells to salivary glands. We found that salivary glands from aged *Lgals1*$^{-/-}$ mice displayed higher *Cxcl9* and *Cxcl10* mRNA expression in comparison to salivary glands from age-matched WT mice (Fig. 3*D*). Consistent with these findings, submandibular lymph nodes (SLNs) from aged *Lgals1*$^{-/-}$ mice showed an increased frequency of total CD8$^+$ and CD8$^+$CXCR3$^+$ T cells (Fig. 3*E*), suggesting that CD8$^+$ effector T cells can be actively recruited to this target organ. Likewise, aged *Mgat5*$^{-/-}$ mice displayed a significantly higher proportion of CD3$^+$CD8$^+$ T cells and a trend toward an increase of CD8$^+$CXCR3$^+$ T cells in SLN compared to WT mice (Fig. 3*F*), suggesting that either lack of Gal1 or of its N-glycosylated ligands could favor recruitment of effector T cells to the target tissue. Thus, Gal1 deficiency facilitates development of an autoimmune inflammatory process in the salivary gland characterized by increased infiltration of IL-2- and IFN-γ–producing PD-1$^+$CD8$^+$ T cells that confront a tissue microenvironment with reduced expression of the inhibitory ligand PD-L1.

Sustained Gal1 Deficiency Interrupts DC-Mediated Regulatory Circuits. Seeking possible mechanisms underlying enhanced CD8$^+$ T-cell effector functions in response to Gal1 deficiency, we analyzed the presence and phenotype of antigen-presenting cells in SLNs. Surprisingly, we found that aged *Lgals1*$^{-/-}$ mice show a reduced number of CD11c$^+$ DCs in SLN when compared to aged WT mice (Fig. 4*A*). However, these cells showed a CD11c^{hi}Ly6C$^-$GR1$^-$CD19$^-$CD8$^-$CD11b$^+$ phenotype and exhibited higher CD86, CD40, and MHC II expression in comparison to DCs from control mice (Fig. 4*B*). Thus, despite their reduced number, DCs displayed a more prominent mature phenotype in

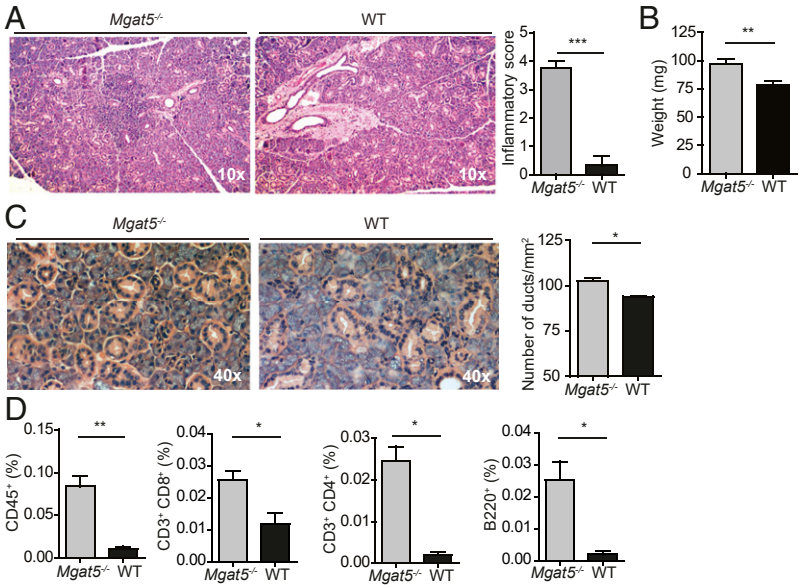

Fig. 2. Interruption of complex N-glycan branching leads to the development of spontaneous sialadenitis. (*A–C*) Analysis of sialadenitis in aged (9 mo) *Mgat5*$^{-/-}$ and WT mice. (*Left*) Representative images of salivary gland tissue sections and (*Right*) inflammatory score (mean ± SEM, $n = 5$; *A*), weight (mean ± SEM, $n = 8$; *B*), and number of ducts per square millimeter (mean ± SEM, $n = 5$; *C*) of submandibular salivary glands. (*D*) Quantification by flow cytometry of the average percentage of infiltrating cell populations of the whole salivary gland of aged (9 mo) *Mgat5*$^{-/-}$ and WT mice (mean ± SEM, $n = 8$). $^{*}P < 0.05$; $^{**}P < 0.01$; $^{***}P < 0.001$, Student's *t* test.

aged Gal1-null mutant mice. To evaluate the functional capacity of these cells, we cocultured DCs from aged *Lgals1*$^{-/-}$ or WT mice with purified CD4^{+} and CD8^{+} T cells from young WT mice. Although aged *Lgals1*$^{-/-}$ and WT DCs showed a comparable capacity of inducing CD8^{+} and CD4^{+} T-cell proliferation (Fig. 4*C*), *Lgals1*$^{-/-}$CD11c^{+} cells induced a bias toward a proinflammatory CD4^{+} T-cell profile characterized by higher IFN-γ and lower IL-10 synthesis compared to that triggered by WT DCs (Fig. 4*D*). However, we found no significant differences in cytokine production by CD8^{+} T cells in coculture experiments with aged CD11c^{+} cells (Fig. 4*E*). We next evaluated the ability of CD11c^{+} cells to promote differentiation of Tregs. Notably, aged *Lgals1*$^{-/-}$ DCs were less effective in promoting differentiation of CD4^{+}CD25^{+}Foxp3^{+} T cells compared to their WT counterpart (Fig. 4*F*). Accordingly, aged *Lgals1*$^{-/-}$ mice showed a reduced percentage of CD4^{+}CD25^{+}Foxp3^{+} and CD4^{+}CTLA-4^{+} cells in SLN as compared to WT mice (Fig. 4*G*). Thus, although CD11c^{+} cells from aged *Lgals1*$^{-/-}$ mice did not differ from WT CD11c^{+} cells in their capacity to induce T-cell proliferation, these cells displayed a lower ability to sustain tolerogenic microenvironments.

Given that salivary gland and lymph nodes from aged *Lgals1*$^{-/-}$ mice display heightened CD8^{+} T-cell effector function, we asked whether enhanced DC immunogenicity, leading to CD4^{+} T-cell activation, may contribute to CD8^{+} T-cell activity. Remarkably, cells and conditioned media obtained from cocultures of DCs and CD4^{+} T cells supported a greater replication of CD8^{+} T cells when CD11c^{+} cells were obtained from aged *Lgals1*$^{-/-}$ mice (Fig. 4*H*). Thus, Gal1-deficient CD11c^{+} DCs display greater immunogenic potential with enhanced T-cell activation properties and reduced capacity to induce Treg cell differentiation.

Gal1 Limits the Severity of Experimental Autoimmune Sialadenitis. To evaluate if variations of endogenous Gal1 synthesis might contribute to the development of autoimmunity in exocrine glands, we analyzed Gal1 expression in salivary glands and serum from nonobese diabetic (NOD) mice, a mouse strain prone to the development of autoimmune sialadenitis and a widely accepted model of Sjögren's syndrome. We found that Gal1 expression decreased with age in serum and salivary glands from NOD mice (Fig. 5 *A* and *B*). Interestingly, this reduction was not observed in BALB/c mice, which did not develop spontaneous autoimmunity (Fig. 5 *C* and *D*). To rescue the autoimmune phenotype, we treated 16-wk-old NOD mice with recombinant Gal1 (rGal1). Administration of rGal1 every 2 d for 2 wk effectively reduced the magnitude of the inflammatory infiltrate in salivary glands, as evidenced by a significant decrease in the frequency of CD45^{+} and CD4^{+} cells and a tendency toward a decline in CD8^{+} and CD19^{+} populations (Fig. 5*G*). Thus, the autoimmune phenotype characterized by reduced Gal1 expression in aged NOD mice can be alleviated by administration of the exogenous recombinant protein.

Lower Gal1 Expression Correlates with Increased CD8^{+} T-Cell Infiltration in Biopsies from Sjögren's Syndrome Patients. To determine the clinical relevance of our findings, we analyzed Gal1 expression in labial biopsies of pSS patients and control subjects (biopsies of individuals with normal labial salivary glands; Table 1). Expression of Gal1 was identified in interstitial areas between acini and ducts of the salivary gland from patients and controls (Fig. 6 *A*, *Left*). Interestingly, biopsies from pSS patients (score IV) showed reduced Gal1^{+} areas as compared to control samples (Fig. 6 *A*, *Right*). Finally, we analyzed the frequency of CD8^{+}, CD20^{+}, and CD4^{+} cell populations in samples from pSS patients. We found a significant negative linear correlation between Gal1^{+} areas and the number of infiltrating CD8^{+} T cells (Fig. 6 *B* and *E*), whereas no significant association was found with the number of CD20^{+} or CD4^{+} cells (Fig. 6 *C*, *D*, *F*, and *G*). Thus, a reduction in Gal1 expression in pSS could account in part for the inflammatory process in salivary glands, suggesting the involvement of this glycan-binding protein in the etiopathogenesis of pSS and highlighting the clinical relevance of our findings.

Discussion

Immune tolerance therapies, including those involving expansion and/or differentiation of tolerogenic DCs and Tregs or amplification of regulatory cytokines, are designed to reprogram immune cells to selectively eliminate pathogenic responses, obviating the

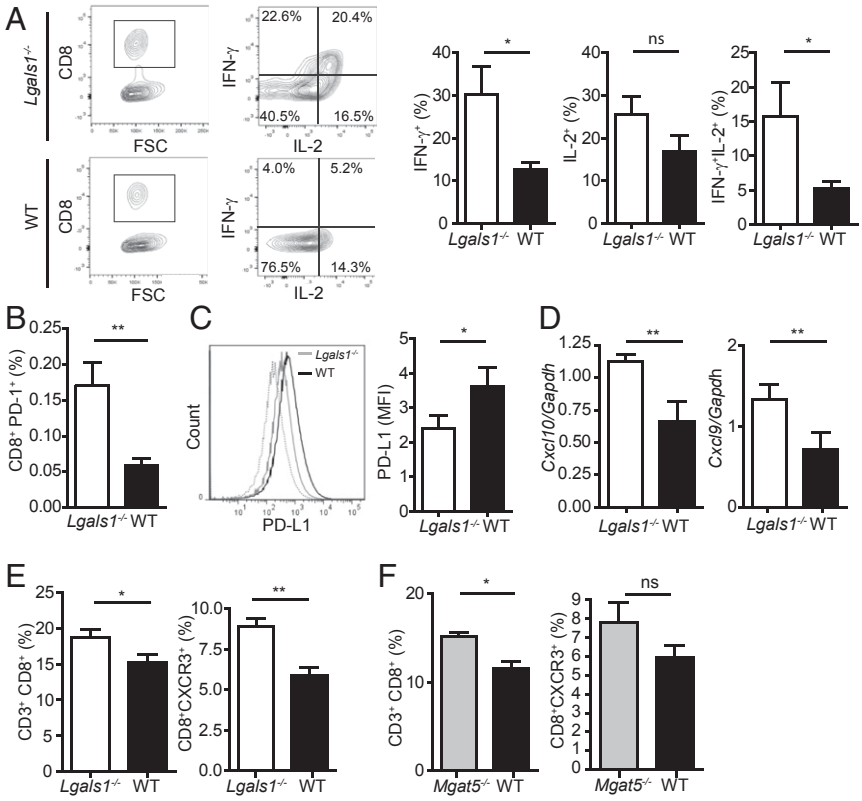

Fig. 3. Gal1 deficiency enhances CD8$^+$ T-cell function in salivary glands. (*A*) Cytokine production by salivary gland-infiltrating CD8$^+$ T cells from aged *Lgals1*$^{-/-}$ and WT mice (9 mo). (*Left*) Representative dot plots and (*Right*) percentage of IFN-γ$^+$, IL-2$^+$, or IFN-γ$^+$IL-2$^+$ CD8$^+$ T cell populations (mean ± SEM, $n = 8$). (*B*) Frequency of CD8$^+$PD-1$^+$ cells on salivary glands of aged (9 mo) *Lgals1*$^{-/-}$ and WT mice (mean ± SEM, $n = 8$; *C*). PD-L1 expression on salivary gland cells from aged *Lgals1*$^{-/-}$ and WT mice (9 mo; mean ± SEM; $n = 8$). (*Right*) Mean fluorescence intensity (MFI) and (*Left*) representative histogram. (*D*) Expression of *Cxcl10* and *Cxcl9* mRNA by RT-qPCR in salivary glands from aged *Lgals1*$^{-/-}$ and WT mice (9 mo; $n = 10$). Results are expressed relative to *Gapdh* mRNA expression. (*E* and *F*) Quantification of the frequency of CD8$^+$ and CD8$^+$CXCR3$^+$ T cells in the submandibular lymph nodes (SLNs) of aged *Lgals1*$^{-/-}$, *Mgat5*$^{-/-}$, and WT mice (9 mo). Comparison between *Lgals1*$^{-/-}$ and WT mice (mean ± SEM, $n = 16$; *E*) and between *Mgat5*$^{-/-}$ and WT mice (mean ± SEM, $n = 8$; *F*). *$P < 0.05$; **$P < 0.01$; ns, nonsignificant; Student's *t* test.

need for generalized immunosuppression (39). We and others have previously shown that glycosylation-dependent Gal1-driven regulatory circuits govern the fate of Th1 and Th17 effector cells (14), promote differentiation of tolerogenic DCs (26, 40), favor polarization of M2 proresolving macrophages and microglia (28, 29, 41), and foster the immunosuppressive activity of Tregs (20, 42, 43). This places Gal1 as an attractive target for the management of a wide range of chronic T-cell–mediated autoimmune diseases.

In this study, we report a central role for endogenous Gal1 as a key immune regulator that promotes immune tolerance and prevents age-dependent spontaneous autoimmunity. The effects of aging in the immune system are widespread and include alterations in immune cell development, activation, and differentiation, leading to impairment of antimicrobial and antitumoral immunity and increased susceptibility to autoimmune inflammation (44). Here we found that aged *Lgals1*$^{-/-}$ mice develop a spontaneous inflammatory disorder similar to Sjögren's syndrome, characterized by increased frequency and activity of CD8$^+$ T cells in lymph nodes and salivary glands.

Studies of immune cell development revealed age-related changes on hematopoietic stem cells, leading to contraction of the lymphoid cell compartment and amplification of myeloid cell programs in both mouse and human (45, 46). We found that Gal1 deficiency increases the frequency of CD8$^+$ T cells in peripheral lymph nodes during aging. Moreover, lack of Gal1 prevents expansion of the myeloid cell compartment as reflected by the reduced percentage of CD11c$^+$ DCs. Hence, inhibition of Gal1 expression recapitulates the young immune phenotype with regard to modulation of lymphoid and myeloid cell compartments. However, despite the lower number of CD11c$^+$ DCs in draining lymph nodes of aged *Lgals1*$^{-/-}$ mice, these cells displayed a more prominent mature phenotype and a greater capacity to induce IFN-γ–mediated responses. Thus, Gal1 deficiency reinforces DC immunogenicity, leading to exuberant tissue-specific autoimmune reactions.

Galectins recognize LacNAc residues in a variety of glycoconjugates containing complex N-glycans and extended O-glycans (47). In particular, the Mgat5 glycosyltransferase synthesizes the β1,6-N-acetylglucosamine branch of complex N-glycans, allowing elongation of repeated LacNAc residues (48). In pioneer studies, Demetriou and colleagues showed that Mgat5 deficiency increases T-cell activation and favors exacerbated immune responses. Accordingly, *Mgat5*$^{-/-}$ mice showed increased frequency of leukocyte colonies in the kidney compatible with autoimmune glomerulonephritis (49). The proposed mechanisms involved reduced binding of Gal3 to T-cell surface glycoproteins, which lowered the threshold of T-cell activation by enhancing T-cell receptor (TCR) clustering (49). In addition, recent studies revealed that metabolic supplementation of mucosal T cells from inflammatory bowel disease patients with N-acetylglucosamine led to increased branched N-glycosylation and inhibition of Th1 and Th17 pathogenic responses (50). Moreover, in mouse models of autoimmune encephalomyelitis and inflammatory bowel disease, Mgat5 deficiency led to increased clinical severity and T-cell–mediated tissue damage in response to inflammatory challenges (50, 51).

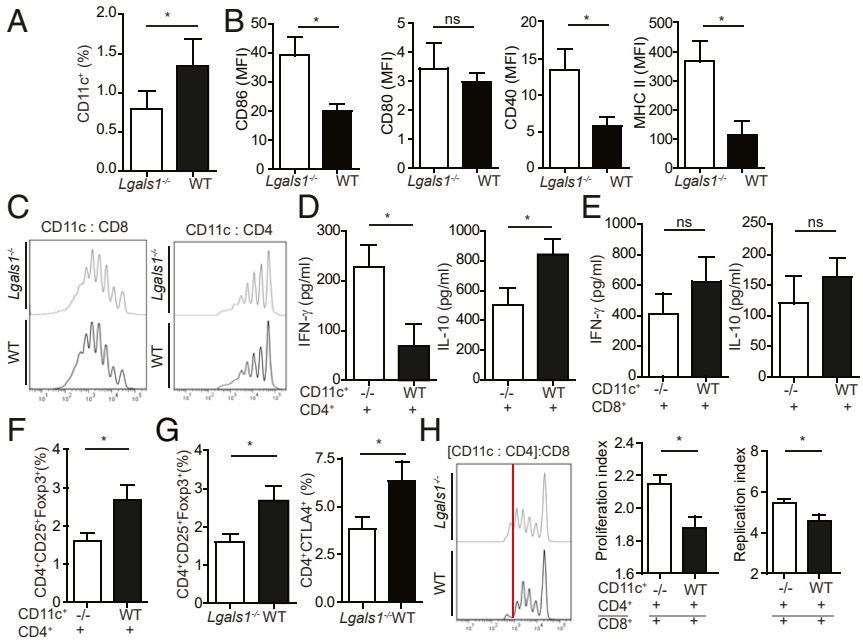

Fig. 4. Gal1 deficiency impairs the tolerogenic capacity of dendritic cells (DCs). (*A* and *B*) Frequency and phenotypic analysis of CD11c$^+$ cells in submandibular lymph nodes (SLNs) of aged (9 mo) *Lgals1*$^{-/-}$ and WT mice. Percentage of CD11c$^+$ cells (mean ± SEM, $n = 8$; *A*). Expression of CD86, CD80, CD40, and MHC II measured as mean fluorescence intensity (MFI; mean ± SEM, $n = 8$; *B*). (*C*–*E*) Cocultures of CD11c$^+$ cells obtained from aged *Lgals1*$^{-/-}$ or WT mice with CD8$^+$ or CD4$^+$ T cells from young WT mice in the presence of an anti-CD3 monoclonal antibody. Representative histograms of CD8 (*Left*) or CD4 (*Right*) T-cell proliferation of five independent experiments with $n = 4$ are shown (*C*). Secretion of IFN-γ and IL-10 in CD11c$^+$:CD4$^+$ (*D*) and CD11c$^+$:CD8$^+$ (*E*) culture supernatants ($n = 7$, mean ± SEM). Frequency of regulatory T cells (Tregs) in CD11c$^+$:CD4$^+$ cocultures ($n = 7$, mean ± SEM; *F*). (*G*) Percentage of CD4$^+$CD25$^+$Foxp3$^+$ Tregs and CD4$^+$CTLA-4$^+$ cells in submandibular lymph nodes (SLNs) of aged (9 mo) *Lgals1*$^{-/-}$ and WT mice ($n = 16$, mean ± SEM). (*H*) Proliferation of CD8$^+$ T cells cultured in the presence of cells and conditioned medium from CD11c$^+$:CD4$^+$ cocultures using *Lgals1*$^{-/-}$ or WT CD11c$^+$ cells. (*Left*) Representative histograms of CD8$^+$ T-cell proliferation measured by CFDA-SE dilution. (*Right*) Proliferation index and replication index ($n = 4$, mean ± SEM; representative results of three independent experiments are shown). *$P < 0.05$; ns, nonsignificant; Student's *t* test.

Interestingly, our study provides a direct comparison of the phenotypes of *Lgals1*$^{-/-}$ and *Mgat5*$^{-/-}$ mice, indicating that both strains develop spontaneous autoimmune sialadenitis. Thus, Gal1 interactions with complex branched N-glycans may function as an immune rheostat that prevents age-dependent spontaneous autoimmunity. However, as compared to *Lgals1*$^{-/-}$, mice lacking Mgat5 display augmented infiltration of all immune cell populations. These observations suggest that additional galectins, including Gal3 and Gal8, may contribute to immune cell homeostasis by interacting with β1,6-branched N-glycans (49, 52). Interestingly, an age-dependent autoimmune phenotype was also observed in mice lacking other endogenous lectins including Siglec-G, a sialic acid-binding lectin, deficiency of which led to elevated autoantibody levels and mild glomerulonephritis (53), and Gal3, absence of which led to a lupus-like disease by promoting spontaneous germinal center formation and autoantibody production (54). Furthermore, loss of liver α2,6-sialyltransferase (ST6Gal1), an enzyme required for α2,6-linked sialylation which prevents Gal1 binding, elicits fatty liver disease characterized by age-dependent buildup of fatty acid droplets and a proinflammatory phenotype involving polarization of M1-type macrophages (55). Altogether, these observations suggest a broader role of endogenous glycan-binding proteins and their glycosylated ligands in supporting immune tolerance in the context of immunological senescence.

In the present study, we found that Gal1 deficiency impacts immune responses by increasing infiltration of a population of activated CD8$^+$PD-1$^+$ T cells in salivary glands and impairing local PD-L1 expression. Further studies should be aimed at examining whether Gal1 directly controls PD-L1 expression on the surface of glandular cells via transcriptional or posttranslational mechanisms or whether this lectin indirectly shapes the local inflammatory response to modulate PD-L1 expression. Accordingly, in tumors, PD-L1 expression can be classified as constitutive or inducible upon T-cell infiltration and IFN-γ production (56, 57). Moreover, PD-L1 expression is increased after IFN-γ exposure in salivary epithelial cells and biopsies of patients with Sjögren's syndrome (58). In our experiments, aged *Lgals1*$^{-/-}$ mice displayed a reduced surface expression of PD-L1 despite exhibiting increased infiltration of CD8$^+$IFN-γ$^+$ cells. Interestingly, both mouse and human PD-L1 have several conserved sites for N-glycosylation, and these glycan structures are required for PD-L1 stability on the cell surface since nonglycosylated PD-L1 has increased turnover rate and degradation as compared to glycosylated forms (59). Regarding our findings, we might hypothesize that interruption of Gal1–N-glycan interactions could reduce cell surface retention of PD-L1, as has been described for the TCR and CTLA-4 (60, 61). Hence, the apparent contradiction of reduced PD-L1 expression in an IFN-γ–enriched microenvironment could be explained by the reduced stability and/or surface retention of PD-L1 due to the absence of galectin–glycan interactions.

Currently, pSS patients are treated with drugs that relieve symptoms, mainly tears and saliva substitutes, topical therapies, sialogogues, and analgesics (62). Systemic therapeutic modalities based on biological products targeting proinflammatory cytokines, antigen presentation, and immune cell activation are currently under study, although with limited results (62, 63). Here, we provide evidence that Gal1 expression is down-regulated during the development of Sjögren's syndrome-like disease in NOD mice and is reduced in gland samples of pSS patients. Moreover, we found a negative linear association between Gal1$^+$ tissue and local infiltration of CD8$^+$ T cells, suggesting that loss of Gal1 may contribute to CD8$^+$ T-cell expansion, recruitment, and amplification of their effector function within the inflammatory microenvironment.

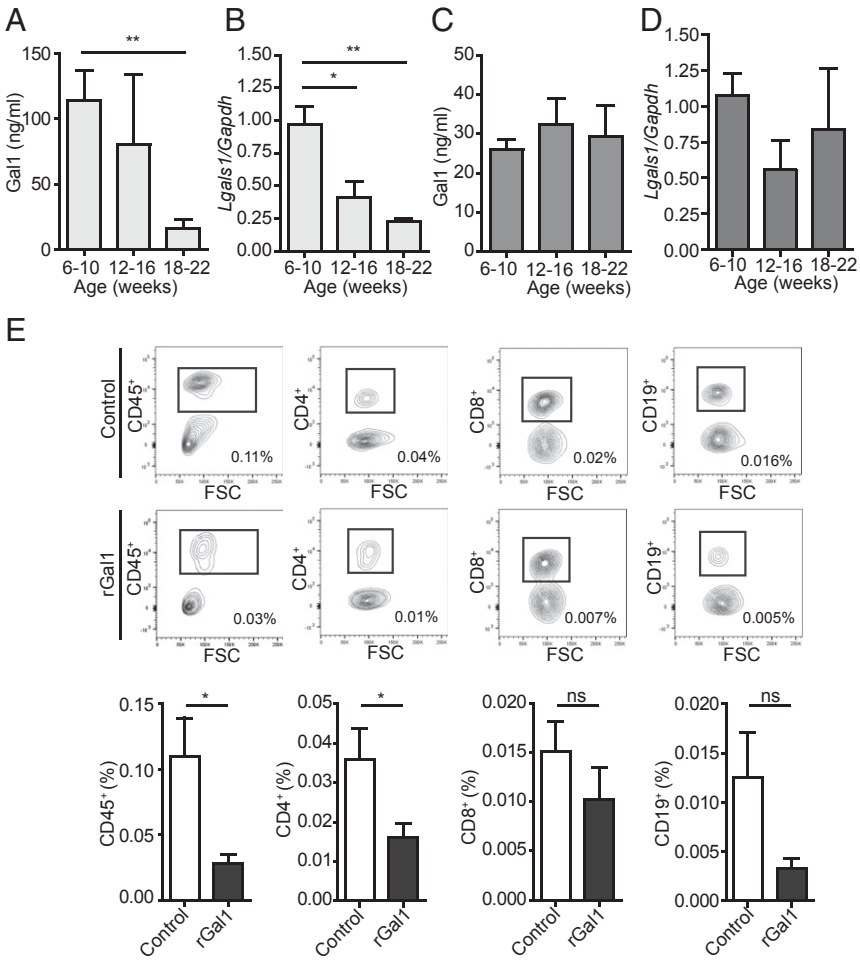

Fig. 5. Age-dependent reduction of Gal1 expression in autoimmune-prone NOD mice. (*A–D*) Determination of Gal1 expression in serum and salivary glands of NOD and BALB/c mice (6 to 10, 12 to 16, and 18 to 22 wk old). ELISA for Gal1 in serum samples of NOD (*A*) and BALB/c (*C*) mice ($n = 5$ per group) and RT-qPCR analysis of Gal1 expression in submandibular salivary glands ($n = 4$ per group) from NOD (*B*) and BALB/c (*D*) mice (*$P < 0.05$; **$P < 0.01$, Student's t test). (*E*) Frequency of infiltrating $CD45^+$, $CD4^+$, $CD8^+$, and $CD19^+$ cells in submandibular salivary glands of NOD (16 wk old) mice treated with rGal1 (100 μg) or PBS (six injections every 2 d). (*Upper*) Representative dot plots showing gating strategies used to quantify the frequency of $CD45^+$, $CD4^+$, $CD8^+$, and $CD19^+$ cells; the value shown on the graph represents the percent value of infiltrating cells with respect to whole salivary gland cells. (*Lower*) The average percentage of infiltrating cell populations with respect to the whole salivary gland (mean ± SEM, $n = 5$). A representative of three independent experiments is shown (*$P < 0.05$, Mann–Whitney test).

Autoantibodies, in addition to autoreactive T cells, play a central role in the pathogenesis of many autoimmune diseases, including rheumatoid arthritis, Sjögren's syndrome, and SLE. In our study, we observed increased serum levels of anti-dsDNA, anti-nuclear, and anti-Ro/SSA antibodies in aged *Lgals1*$^{-/-}$ mice. These results emphasize the broader role of Gal1–N-glycan interactions in suppressing autoimmune inflammation, consistent with previous studies reporting the ability of rGal1 to inhibit production of anti-dsDNA autoantibodies and reducing proteinuria in experimental lupus-like disease (*NZBxNZW* mice) (31). Interestingly, aged *Lgals1*$^{-/-}$ mice of the 129S/V background had a significant increase in anti-dsDNA autoantibodies (31). Here we show that Gal1 deficiency promotes the emergence of autoantibodies that could be involved in both Sjögren's syndrome and lupus-like diseases; however, in our experimental conditions, we found no overt kidney damage in aged *Lgals1*$^{-/-}$ mice (*SI Appendix*, Fig. S1), suggesting that genetic background and environmental factors may determine the clinical outcome of different autoimmune diseases. Finally, we demonstrate that administration of rGal1 to NOD mice with compromised salivary gland autoimmunity attenuates immune cell infiltration. Given the limitations encountered in treatment of this complex autoimmune disease and the urgent need for more selective therapies, Gal1-based immunomodulatory drugs may be effective either alone or in combination to reduce disease severity and improve life quality of pSS patients.

Materials and Methods

Mouse. *Lgals1*$^{-/-}$ mice were originally provided by Francoise Poirier (Institut Jacques Monod, Paris, France). *Mgat5*$^{-/-}$, NOD, C57BL/6 WT, and BALB/c mice

Table 1. Characteristics and clinical features of patients with primary Sjögren's syndrome (pSS) and control subjects

Characteristic	pSS patients	Control subjects
No. of patients	19	14
Inflammatory score	III/IV	0
Sex	15 (F); 4 (M)	12 (F); 2 (M)
Age, y	52 ± 8	43 ± 11
Time after diagnosis, y	4 ± 5	—
Xerostomy	17/19	14/14
+Anti-Ro	14/19	3/14
+Anti-La	9/19	3/14

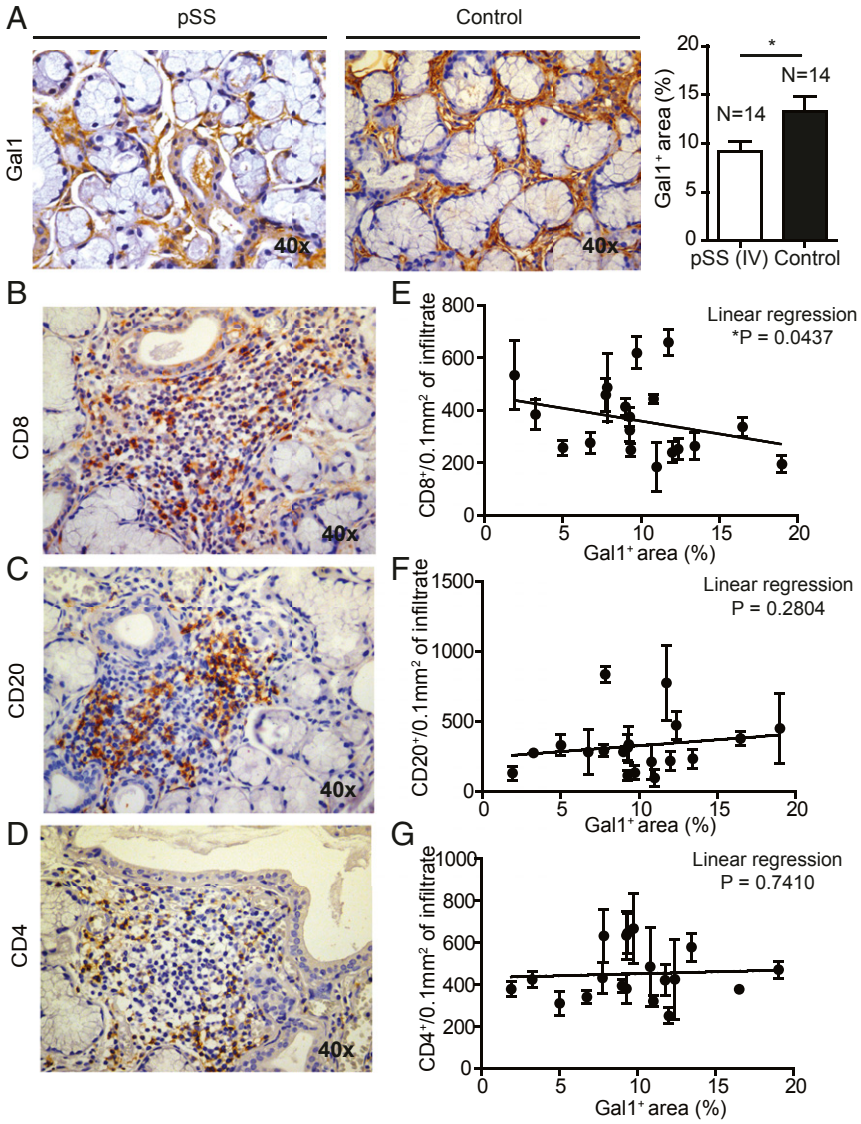

Fig. 6. Dysregulated Gal1 expression in salivary glands from primary Sjögren's syndrome patients. (*A*) Detection of Gal1 by immunohistochemistry in labial biopsies from pSS patients and control individuals (suspected sialadenitis with negative biopsies; score 0). (*Left*) Representative images used to quantify the Gal1$^+$ area. (*Right*) Quantification (mean ± SEM of Gal1$^+$ area; *$P < 0.05$, Student's *t* test). (*B–D*) Immunohistochemical analysis of CD8$^+$, CD20$^+$, and CD4$^+$ cells in labial biopsies of pSS patients. (*E–G*) Linear regression between Gal1$^+$ area and the number of CD8$^+$ (*E*), CD20$^+$ (*F*), and CD4$^+$ (*G*); $n = 19$; *$P < 0.05$, linear regression.

were provided by The Jackson Laboratory. Animals (female mice) were bred at the animal facilities of the Institute of Biology and Experimental Medicine and the School of Exact and Natural Sciences (University of Buenos Aires) according to National Institutes of Health guidelines. This included ages 8 to 12 wk (young C57BL/6 WT mice), ≥9 mo (aged *Lgals1*$^{-/-}$, *Mgat5*$^{-/-}$, and C57BL/6 WT mice), and 6 to 22 wk (NOD and BALB/c mice). All experimental procedures were reviewed and approved by the institutional animal care and use committee.

ELISA. Measurements of anti-dsDNA, anti-ANA, and anti-SSA/Ro60 were performed according to the manufacturer's instructions (Alpha Diagnostic) in serum samples of *Lgals1*$^{-/-}$ and WT mice. Mouse IFN-γ and IL-10 were determined in culture supernatants using a DuoSet enzyme-linked immunosorbent assay (ELISA) kit (R&D Systems) and an ELISA set (BD OptEIA), respectively. Soluble Gal1 was determined in serum samples of NOD and WT mice using an in-house ELISA as previously described (64). In brief, high-binding 96-well microplates (Costar; Corning) were coated with purified rabbit anti-mouse Gal1 polyclonal IgG (2 μg/mL), blocked with 2% BSA in PBS, detected with biotinylated anti-Gal1 polyclonal IgG (100 ng/mL), and revealed using 0.1 mg/mL tetramethylbenzidine and 0.06% H_2O_2 in citrate phosphate buffer, pH 5.0. Optical densities were determined at 450 nm and 550 nm in a Multiskan MS microplate reader (Thermo Fisher Scientific). A standard curve ranging from 2.5 to 160 ng/mL rGal1 was run in parallel.

Indirect Immunofluorescence in HEp-2 Cells. Autoantibodies were detected using an adapted protocol of indirect immunofluorescence in HEp-2 cells (BioSystems). Briefly, diluted serum samples (1:80) were incubated with adherent HEp-2 cells ($n = 6$ wells per slide). After 30 min incubation, slides were washed and incubated with Alexa Fluor 488-conjugated anti-mouse IgG (1:1,000; Cell Signaling) and Evans blue counterstain (Sigma Diagnostics) for an additional 30 min. Examination was performed using confocal microscopy (Fluoview10i; Olympus). The pattern was determined according to the manufacturer's instructions. The nuclear green fluorescence intensity was quantified using ImageJ program (v1.64).

Histopathology. Submandibular glands as well as other organs (kidney, skin, stomach, retina, thyroid, pancreas, liver, and uterus) were fixed in 4% paraformaldehyde and embedded in paraffin. Tissue sections stained with hematoxylin–eosin were used for histopathological assessment. The inflammatory score for salivary glands was determined according to histopathological

diagnosis criteria established by Chisholm and Mason (38). In brief, grade 0, without infiltrate; grade I, mild diffuse lymphocytic/plasmacytic infiltrate; grade II, moderate infiltrate or less than one focus of 50 mononuclear cells per 4 mm^2; grade III, one focus of 50 mononuclear cells per 4 mm^2; grade IV, more than one focus of 50 mononuclear cells per 4 mm^2. The number of ducts per area was determined by counting four random fields per gland using 40× images and the ImageJ program (v1.64).

Cell Suspensions and Flow Cytometry. Cell suspensions from submandibular glands were generated using a gentleMACS Dissociator (Miltenyi Biotec). Lymph node and spleen cell suspensions were obtained by mechanic disruption. Red blood cells were lysed and all suspensions filtered. Cell surface staining was performed using several combinations of antibodies: PE-conjugated anti-CD45, PE-conjugated anti-CD8, FITC-conjugated anti-CD3, APC-conjugated anti-CD4, APC-conjugated anti-CD45R (B220), PE-conjugated anti-CD11c, APC-conjugated anti-CXCR3, FITC-conjugated anti-CD8, PercP-Cy5,5-conjugated anti–PD-1, PE-conjugated anti–PD-L1, APC-conjugated anti–CTLA-4, PE-conjugated anti-CD86, PE-conjugated anti-MHC II, FITC-conjugated anti-CD4, PE-conjugated anti-CD25, PECy7-conjugated anti-CD19 (all from BD Biosciences), FITC-conjugated anti-CD80 (Biolegend) and FITC-conjugated anti-CD40 (Novus Biologicals). Frequency of Tregs was determined using the mouse Treg staining kit (eBioscience) and the antibody APC-conjugated anti-mouse Foxp3 (BD Biosciences). For determination of intracellular cytokines, cells were cultured with ionomycin (750 ng/mL; Sigma) and PMA (50 ng/mL; Sigma) for 5 h. GolgiStop (BD Biosciences) was added after 1 h. Cell surface staining was performed before fixation and permeabilization using BD Cytofix/Cytoperm (BD Biosciences). Intracellular staining was performed with FITC-conjugated anti–IFN-γ and PeCy7-conjugated anti–IL-2 (BD Biosciences). Samples were analyzed on a FACSCanto (BD Biosciences) with FlowJo software (v7.6.5).

Real-Time Quantitative RT-PCR. RNA was obtained using TRIzol reagent according to the manufacturer's instructions. DNA contamination was removed using DNase I. cDNA was synthesized using SuperScript III Reverse Transcriptase (Invitrogen). For real-time PCR, the SYBR Green PCR Master Mix was used with an ABI System 7500 (Applied Biosystem). Primers are as follows: *Lgals1* 5′-TCAGCCTGGTCAAAGGTGAT-3′ 5′-TGAACCTGGGAAAAGACAGC-3′, *Cxcl10* 5′-ATGACGGGCCAGTGAGAATG-3′ 5′-TCGTGGCAATGATCTCAACAC-3′, *Cxcl9* 5′-TCGGACTTCACTCCAACACAG-3′ 5′-AGGGTTCCTCGAACTCCACA-3′, and *Gapdh* 5′-CAGAACATCATCCCTGCAT-3′ 5′-GTTCAGCTCTGGGATGACCTT-3′. Quantification was performed as an absolute value using *Gapdh* as a housekeeping gene.

Coculture of DCs and T Cells. $CD4^+$ and $CD8^+$ T lymphocytes from 8- to 12-wk-old WT mice were isolated using Dynabeads untouched Mouse CD4 cells kit and Dynabeads untouched mouse CD8 cells kit (both from Invitrogen), respectively. $CD11c^+$ cells of 9-mo-old *Lgals1*$^{-/-}$ or WT mice were purified by cell sorting using a FACSAria II (BD Biosciences) or using mouse CD11c microbeads (Miltenyi Biotec). Cocultures of $CD4^+$:$CD11c^+$ cells and $CD8^+$:$CD11c^+$ cells (10:1) were performed in RPMI 10% serum (Gibco) and antibiotic-antimycotic (Gibco) with soluble purified NA/LE anti-mouse CD3e (1 μg/mL; BD Biosciences) in 96-well U-plates for 96 h. In another set of experiments, 1×10^5 cells from the $CD4^+$:$CD11c^+$ cocultures were taken and incubated with 1×10^5 $CD8^+$ T cells in the presence of $CD4^+$:$CD11c^+$ conditioned medium (1:1), soluble purified NA/LE anti-mouse CD3e (1 μg/mL; BD Biosciences), and purified NA/LE anti-mouse CD28 (2 μg/mL; BD Biosciences) antibodies for 72 h.

Proliferation Assay. Purified $CD4^+$ and $CD8^+$ cells were labeled using Vybrant CFDA-SE cell tracer kit (Molecular Probes) before coculture experiments. Briefly, cells were washed with PBS and incubated with CFDA-SE (1.5 μM) for 7 min at 37 °C. Proliferation was analyzed on a FACSCanto (BD Biosciences) using the proliferation tool of FlowJo software (v7.6.5), obtaining proliferation and replication indexes.

Labial Biopsies of pSS Patients. Human paraffin-embedded labial biopsies of patients with pSS (inflammatory score III/IV) and controls (suspected sialadenitis with negative biopsies; score 0) were provided by the Rheumatology Unit from Hospital Bernardino Rivadavia (Buenos Aires, Argentina). Complementary information is shown in Table 1. Samples were obtained following patients' informed consent, and protocols were approved by the ethics committee of Hospital Rivadavia.

Immunohistochemistry. Sections from labial biopsy samples (5 μm) were dewaxed and rehydrated in serial ethanol dilutions. Endogenous peroxidase activity was blocked with 3% H_2O_2. Antigen retrieval was performed with sodium citrate treatment (0.01 M; pH 6.0), and nonspecific antigens were blocked with horse serum. Slides were stained with anti-human Gal1, anti-human CD8, anti-human CD4, and anti-human CD20 antibodies. Primary antibodies (1:100; Abcam) were incubated overnight and detected using the Vectastain ELITE ABC kit (Vector Lab). Micrographs were taken with an Olympus CX31 microscope and analyzed using ImageJ software (v1.64).

Treatment with rGal1. Sixteen-week-old NOD mice were treated with rGal1 (100 μg per mouse; i.p.) or PBS three times a week for 2 wk as described (16). Animals were euthanized, salivary glands processed, and cell suspensions were stained and revealed by flow cytometry as previously described.

Statistical Analysis. Prism 5.0 software (GraphPad) was used for statistical analysis. Two groups were compared with the Student's *t* test or Mann–Whitney test for unpaired data, and lineal relations were tested with lineal regression statistics. *P* values of 0.05 or less were considered significant.

Data Availability. All data, associated protocols, and materials used for this study are available within the manuscript and *SI Appendix*.

ACKNOWLEDGMENTS. We thank P. Hockl and S. Maller for technical assistance; and J. Ilarregui and A. Blidner for advice. This work was supported by grants from Agencia Nacional de Promoción Científica y Tecnológica (PICT 2013-0919 to M.A.T., and PICT 2010-870 and 2014-3687 to G.A.R.); Consejo Nacional de Investigaciones Científicas y Técnicas (PIP-CONICET 041/13 to M.A.T. and PIP-CONICET 0672/12 to C.P.L.); as well as grants from Bunge & Born, Sales, and Richard Lounsbery Foundations (to G.A.R.). We thank the Ferioli, Ostry, and Caraballo families for generous donations. We thank Marcos Barboza for his collaboration with the G.A.R. laboratory during his life.

1. J. A. Bluestone, H. Bour-Jordan, M. Cheng, M. Anderson, T cells in the control of organ-specific autoimmunity. *J. Clin. Invest.* **125**, 2250–2260 (2015).
2. N. Joller, A. Peters, A. C. Anderson, V. K. Kuchroo, Immune checkpoints in central nervous system autoimmunity. *Immunol. Rev.* **248**, 122–139 (2012).
3. C. A. Chambers, T. J. Sullivan, J. P. Allison, Lymphoproliferation in CTLA-4-deficient mice is mediated by costimulation-dependent activation of CD4+ T cells. *Immunity* **7**, 885–895 (1997).
4. B. Zhang, S. Chikuma, S. Hori, S. Fagarasan, T. Honjo, Nonoverlapping roles of PD-1 and FoxP3 in maintaining immune tolerance in a novel autoimmune pancreatitis mouse model. *Proc. Natl. Acad. Sci. U.S.A.* **113**, 8490–8495 (2016).
5. A. B. Kulkarni *et al*., Transforming growth factor beta 1 null mutation in mice causes excessive inflammatory response and early death. *Proc. Natl. Acad. Sci. U.S.A.* **90**, 770–774 (1993).
6. H. Nishimura, M. Nose, H. Hiai, N. Minato, T. Honjo, Development of lupus-like autoimmune diseases by disruption of the PD-1 gene encoding an ITIM motif-carrying immunoreceptor. *Immunity* **11**, 141–151 (1999).
7. H. Nishimura *et al*., Autoimmune dilated cardiomyopathy in PD-1 receptor-deficient mice. *Science* **291**, 319–322 (2001).
8. Y. Oya *et al*., Development of autoimmune hepatitis-like disease and production of autoantibodies to nuclear antigens in mice lacking B and T lymphocyte attenuator. *Arthritis Rheum.* **58**, 2498–2510 (2008).
9. R. Y. Yang, G. A. Rabinovich, F.-T. Liu, Galectins: Structure, function and therapeutic potential. *Expert Rev. Mol. Med.* **10**, e17 (2008).
10. J. P. Cerliani, A. G. Blidner, M. A. Toscano, D. O. Croci, G. A. Rabinovich, Translating the 'sugar code' into immune and vascular signaling programs. *Trends Biochem. Sci.* **42**, 255–273 (2017).
11. M. A. Toscano, V. C. Martínez Allo, A. M. Cutine, G. A. Rabinovich, K. V. Mariño, Untangling galectin-driven regulatory circuits in autoimmune inflammation. *Trends Mol. Med.* **24**, 348–363 (2018).
12. G. A. Rabinovich, D. O. Croci, Regulatory circuits mediated by lectin-glycan interactions in autoimmunity and cancer. *Immunity* **36**, 322–335 (2012).
13. S. Thiemann, L. G. Baum, Galectins and immune responses–Just how do they do those things they do? *Annu. Rev. Immunol.* **34**, 243–264 (2016).
14. M. A. Toscano *et al*., Differential glycosylation of TH1, TH2 and TH-17 effector cells selectively regulates susceptibility to cell death. *Nat. Immunol.* **8**, 825–834 (2007).
15. H. Offner *et al*., Recombinant human beta-galactoside binding lectin suppresses clinical and histological signs of experimental autoimmune encephalomyelitis. *J. Neuroimmunol.* **28**, 177–184 (1990).
16. G. A. Rabinovich *et al*., Recombinant galectin-1 and its genetic delivery suppress collagen-induced arthritis via T cell apoptosis. *J. Exp. Med.* **190**, 385–398 (1999).
17. L. Santucci *et al*., Galectin-1 exerts immunomodulatory and protective effects on concanavalin A-induced hepatitis in mice. *Hepatology* **31**, 399–406 (2000).
18. L. Santucci *et al*., Galectin-1 suppresses experimental colitis in mice. *Gastroenterology* **124**, 1381–1394 (2003).
19. Y. Tsuchiyama *et al*., Efficacy of galectins in the amelioration of nephrotoxic serum nephritis in Wistar Kyoto rats. *Kidney Int.* **58**, 1941–1952 (2000).

20. M. A. Toscano *et al*., Galectin-1 suppresses autoimmune retinal disease by promoting concomitant Th2- and T regulatory-mediated anti-inflammatory responses. *J. Immunol.* **176**, 6323–6332 (2006).
21. M. J. Perone *et al*., Suppression of autoimmune diabetes by soluble galectin-1. *J. Immunol.* **182**, 2641–2653 (2009).
22. C. V. Pérez *et al*., Dual roles of endogenous and exogenous galectin-1 in the control of testicular immunopathology. *Sci. Rep.* **5**, 12259 (2015).
23. N. L. Perillo, K. E. Pace, J. J. Seilhamer, L. G. Baum, Apoptosis of T cells mediated by galectin-1. *Nature* **378**, 736–739 (1995).
24. G. A. Rabinovich *et al*., Activated rat macrophages produce a galectin-1-like protein that induces apoptosis of T cells: Biochemical and functional characterization. *J. Immunol.* **160**, 4831–4840 (1998).
25. K. E. Pace, H. P. Hahn, M. Pang, J. T. Nguyen, L. G. Baum, CD7 delivers a pro-apoptotic signal during galectin-1-induced T cell death. *J. Immunol.* **165**, 2331–2334 (2000).
26. J. M. Ilarregui *et al*., Tolerogenic signals delivered by dendritic cells to T cells through a galectin-1-driven immunoregulatory circuit involving interleukin 27 and interleukin 10. *Nat. Immunol.* **10**, 981–991 (2009).
27. S. R. Stowell *et al*., Galectin-1 induces reversible phosphatidylserine exposure at the plasma membrane. *Mol. Biol. Cell* **20**, 1408–1418 (2009).
28. P. Barrionuevo *et al*., A novel function for galectin-1 at the crossroad of innate and adaptive immunity: Galectin-1 regulates monocyte/macrophage physiology through a nonapoptotic ERK-dependent pathway. *J. Immunol.* **178**, 436–445 (2007).
29. S. C. Starossom *et al*., Galectin-1 deactivates classically activated microglia and protects from inflammation-induced neurodegeneration. *Immunity* **37**, 249–263 (2012).
30. A. J. Iqbal *et al*., Endogenous galectin-1 exerts tonic inhibition on experimental arthritis. *J. Immunol.* **191**, 171–177 (2013).
31. S. D. Liu *et al*., Galectin-1-induced down-regulation of T lymphocyte activation protects (NZB x NZW) F1 mice from lupus-like disease. *Lupus* **20**, 473–484 (2011).
32. C. P. Mavragani, H. M. Moutsopoulos, The geoepidemiology of Sjögren's syndrome. *Autoimmun. Rev.* **9**, A305–A310 (2010).
33. D. Cornec, C. Jamin, J. O. Pers, Sjögren's syndrome: Where do we stand, and where shall we go? *J. Autoimmun.* **51**, 109–114 (2014).
34. B. A. Fisher *et al*.; Sjögren's histopathology workshop group (appendix) from ESSENTIAL (EULAR Sjögren's syndrome study group), Standardisation of labial salivary gland histopathology in clinical trials in primary Sjögren's syndrome. *Ann. Rheum. Dis.* **76**, 1161–1168 (2017).
35. F. Ferro, E. Marcucci, M. Orlandi, C. Baldini, E. Bartoloni-Bocci, One year in review 2017: Primary Sjögren's syndrome. *Clin. Exp. Rheumatol.* **35**, 179–191 (2017).
36. R. Jonsson *et al*., The complexity of Sjögren's syndrome: Novel aspects on pathogenesis. *Immunol. Lett.* **141**, 1–9 (2011).
37. M. Voulgarelis, A. G. Tzioufas, Pathogenetic mechanisms in the initiation and perpetuation of Sjögren's syndrome. *Nat. Rev. Rheumatol.* **6**, 529–537 (2010).
38. D. M. Chisholm, D. K. Mason, Labial salivary gland biopsy in Sjögren's disease. *J. Clin. Pathol.* **21**, 656–660 (1968).
39. L. M. R. Ferreira, Y. D. Muller, J. A. Bluestone, Q. Tang, Next-generation regulatory T cell therapy. *Nat. Rev. Drug Discov.* **18**, 749–769 (2019).
40. C. V. Poncini *et al*., *Trypanosoma cruzi* infection imparts a regulatory program in dendritic cells and T cells via galectin-1-dependent mechanisms. *J. Immunol.* **195**, 3311–3324 (2015).
41. R. Rostoker *et al*., Galectin-1 induces 12/15-lipoxygenase expression in murine macrophages and favors their conversion toward a pro-resolving phenotype. *Prostaglandins Other Lipid Mediat.* **107**, 85–94 (2013).
42. T. Dalotto-Moreno *et al*., Targeting galectin-1 overcomes breast cancer-associated immunosuppression and prevents metastatic disease. *Cancer Res.* **73**, 1107–1117 (2013).
43. M. I. Garín *et al*., Galectin-1: A key effector of regulation mediated by CD4+CD25+ T cells. *Blood* **109**, 2058–2065 (2007).
44. J. J. Goronzy, C. M. Weyand, Understanding immunosenescence to improve responses to vaccines. *Nat. Immunol.* **14**, 428–436 (2013).
45. E. Montecino-Rodriguez, B. Berent-Maoz, K. Dorshkind, Causes, consequences, and reversal of immune system aging. *J. Clin. Invest.* **123**, 958–965 (2013).
46. D. J. Rossi *et al*., Cell intrinsic alterations underlie hematopoietic stem cell aging. *Proc. Natl. Acad. Sci. U.S.A.* **102**, 9194–9199 (2005).
47. R. D. Cummings, F.-T. Liu, G. R. Vasta, "Galectins" in *Essentials of Glycobiology*, A. Varki *et al*., Eds. (Cold Spring Harbor Laboratory Press, Cold Spring Harbor, NY, 2015), pp. 469–480.
48. P. Stanley, N. Taniguchi, M. Aebi, "N-Glycans" in *Essentials of Glycobiology*, A. Varki *et al*., Eds. (Cold Spring Harbor Laboratory Press, Cold Spring Harbor, NY, 2015), pp. 99–111.
49. M. Demetriou, M. Granovsky, S. Quaggin, J. W. Dennis, Negative regulation of T-cell activation and autoimmunity by Mgat5 N-glycosylation. *Nature* **409**, 733–739 (2001).
50. A. M. Dias *et al*., Metabolic control of T cell immune response through glycans in inflammatory bowel disease. *Proc. Natl. Acad. Sci. U.S.A.* **115**, E4651–E4660 (2018).
51. S. U. Lee *et al*., N-glycan processing deficiency promotes spontaneous inflammatory demyelination and neurodegeneration. *J. Biol. Chem.* **282**, 33725–33734 (2007).
52. J. F. Sampson *et al*., Galectin-8 ameliorates murine autoimmune ocular pathology and promotes a regulatory T-cell response. *PLoS One* **10**, e0130772 (2015).
53. J. Müller *et al*., Siglec-G deficiency leads to autoimmunity in aging C57BL/6 mice. *J. Immunol.* **195**, 51–60 (2015).
54. C. G. Beccaria *et al*., Galectin-3 deficiency drives lupus-like disease by promoting spontaneous germinal centers formation via IFN-γ. *Nat. Commun.* **9**, 1628 (2018).
55. D. M. Oswald, M. B. Jones, B. A. Cobb, Modulation of hepatocyte sialylation drives spontaneous fatty liver disease and inflammation. *Glycobiology*, 10.1093/glycob/cwz096 (2019).
56. A. Ribas, S. Hu-Lieskovan, What does PD-L1 positive or negative mean? *J. Exp. Med.* **213**, 2835–2840 (2016).
57. P. C. Tumeh *et al*., PD-1 blockade induces responses by inhibiting adaptive immune resistance. *Nature* **515**, 568–571 (2014).
58. M. Kobayashi *et al*., Enhanced expression of programmed death-1 (PD-1)/PD-L1 in salivary glands of patients with Sjögren's syndrome. *J. Rheumatol.* **32**, 2156–2163 (2005).
59. C. W. Li *et al*., Glycosylation and stabilization of programmed death ligand-1 suppresses T-cell activity. *Nat. Commun.* **7**, 12632 (2016).
60. K. S. Lau *et al*., Complex N-glycan number and degree of branching cooperate to regulate cell proliferation and differentiation. *Cell* **129**, 123–134 (2007).
61. M. Takahashi, Y. Hasegawa, C. Gao, Y. Kuroki, N. Taniguchi, N-glycans of growth factor receptors: Their role in receptor function and disease implications. *Clin. Sci. (Lond.)* **130**, 1781–1792 (2016).
62. M. Ramos-Casals *et al*.; EULAR-Sjögren Syndrome Task Force Group, EULAR recommendations for the management of Sjögren's syndrome with topical and systemic therapies. *Ann. Rheum. Dis.* **79**, 3–18 (2020).
63. C. P. Mavragani, H. M. Moutsopoulos, Sjögren's syndrome: Old and new therapeutic targets. *J. Autoimmun.* **9**, 102364 (2019).
64. D. O. Croci *et al*., Disrupting galectin-1 interactions with N-glycans suppresses hypoxia-driven angiogenesis and tumorigenesis in Kaposi's sarcoma. *J. Exp. Med.* **209**, 1985–2000 (2012).